Journal of Alloys and Compounds 504S (2010) S328–S331

Contents lists available at ScienceDirect

Journal of Alloys and Compounds

journal homepage: www.elsevier.com/locate/jallcom

Surface modification of $Mg_{95}Zn_{4.3}Y_{0.7}$ alloy powder consolidates by plasma electrolytic oxidation

Kang M. Lee[a], In J. Hwang[a], Taek-Soo Kim[b], Bongyoung Yoo[a], Dong H. Shin[a,*]

[a] Department of Metallurgy and Materials Science, Hanyang University, Ansan 426-791, Republic of Korea
[b] Center for Echo-Materials and Processing, Korea Institute of Industrial Technology, Incheon 406-840, Republic of Korea

ARTICLE INFO

Article history:
Received 6 July 2009
Received in revised form 9 February 2010
Accepted 19 February 2010
Available online 3 March 2010

Keywords:
Plasma electrolytic oxidation
Mg alloy
Corrosion resistance
Powder consolidates

ABSTRACT

This work investigates the microstructure and corrosion resistance of the oxide layer on $Mg_{95}Zn_{4.3}Y_{0.7}$ alloy powder consolidates prepared by plasma electrolytic oxidation (PEO). The oxide layers on the $Mg_{95}Zn_{4.3}Y_{0.7}$ alloy samples exhibited surface morphology typical of bulk Mg and Mg alloys treated using the PEO process, regardless of the thickness of the layer. The polarization resistance of the oxide layer increased as the thickness of the layer increased. The best corrosion resistance was obtained for the sample with a 30 μm oxide layer. All samples were produced using an electrolyte containing $K_4P_2O_7$. A reasonable equivalent circuit to analyze the corrosion behavior of $Mg_{95}Zn_{4.3}Y_{0.7}$ alloy was established, and the fitting results were consistent with the results of electrochemical impedance spectroscopy (EIS) testing. These results explain the relationship of enhanced corrosion resistance to the thickness of oxide layer in environments containing Cl^- ions.

1. Introduction

Mg alloys have a superior strength-to-weight ratio, higher dimensional stability, lower density and better electromagnetic shielding than several other alloys. For these excellent physical and mechanical properties, Mg alloys have been used in many applications, such as mobile electronics, aerospace products, computers, and household equipment. Unfortunately, magnesium alloys have poor corrosion resistance, especially in acidic environments and in conditions where exposed to salt-water [1].

In recent years, it has been found that an addition of rare-earth elements, especially yttrium, to Mg alloys can improve both the low and high temperature strength of such alloys [2,3]. In Mg alloys, a small addition of yttrium is effective to modify the low flowability, the microstructure, the ambient and high temperature mechanical properties, and the corrosion resistance of these alloys [4–7]. Additionally, it was reported that Mg alloys, especially $Mg_{95}Zn_{4.3}Y_{0.7}$, fabricated by the powder metallurgy (PM) process yielded better performances [8]. However, Mg alloys produced by the PM process need additional treatment to improve their corrosion resistance due to the fact that such alloys are still active in ambient environments.

Plasma electrolytic oxidation (PEO) is one of the most attractive surface treatment methods for Mg alloys, and forms an oxide layer on Mg alloy in the plasma state generated by applying extremely high voltage to the alloy in a suitable electrolyte [9,10]. The surface structures formed during the PEO process depend on various processing conditions, including the chemical composition and concentration of the electrolyte, the current density, and the alloy composition of the substrate. The chemical composition of the electrolyte used in the PEO process exerts a particularly important influence on the formation of final properties of the oxide coating on Mg alloys. Additives such as phosphate, fluoride, and borate are commonly used in the PEO process for Mg alloys [11]. However, most studies to improve corrosion resistance have concentrated on bulk Mg and Mg alloys and have been devoted to exploring the effects of processing parameters such as composition, electrolyte concentration, and electric variables. As a result, there is still a lack of information on the corrosion resistance of the plasma-anodized oxide layer on $Mg_{95}Zn_{4.3}Y_{0.7}$ alloy prepared using the PM process. In this study, $Mg_{95}Zn_{4.3}Y_{0.7}$ alloy prepared via direct extrusion after gas atomization was processed by PEO to improve its corrosion resistance, and the corrosion behavior of the oxide layer formed on the $Mg_{95}Zn_{4.3}Y_{0.7}$ alloy was evaluated by electrochemical analysis.

2. Experimental procedure

$Mg_{95}Zn_{4.3}Y_{0.7}$ alloy extruded with an extrusion ratio of 15:1 at 623 K and a ram speed of 1 mm/s was used in this study. $Mg_{95}Zn_{4.3}Y_{0.7}$ alloy cylinders with 10 mm in diameter and 2 mm in height were mechanically prepared for the PEO process. Stainless steel was used as the counter electrode in an electrolyte containing 0.12 M KOH + 0.05 M KF + 0.02 M Na_2SiO_3 + 0.02 M $K_4P_2O_7$, and the stirring and cooling system were set up to maintain the temperature of the electrolyte at 293–303 K during the PEO process. The applied current density was maintained at

* Corresponding author.
E-mail address: dhshin@hanyang.ac.kr (D.H. Shin).

0925-8388/$ – see front matter © 2010 Elsevier B.V. All rights reserved.
doi:10.1016/j.jallcom.2010.02.146

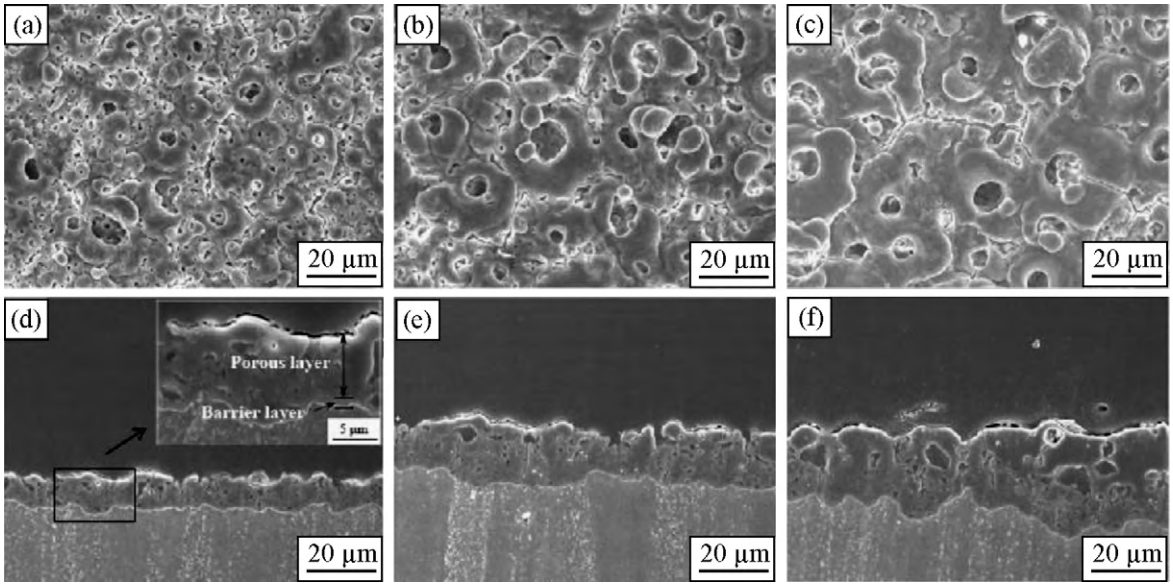

Fig. 1. Morphologies of oxide layers on PM-processed $Mg_{95}Zn_{4.3}Y_{0.7}$ alloy synthesized by the PEO process; surface images: (a) 10 μm, (b) 20 μm, (c) 30 μm, and cross-sectional images: (d) 10 μm, (e) 20 μm, (f) 30 μm.

50 mA/cm^2. The surface morphology and cross-sectional images of the oxide layer were observed using a scanning electron microscope (HITACHI, S-4800) and energy-dispersive spectroscopy (EDS) was conducted to examine the constituent elements in the oxide layer. The phase composition of coatings was determined by using X-ray diffraction (XRD, RIGAKU, D MAX-2500) with a step size 0.02° and a scan range from 20° to 80°. Spectra were recorded using Cu Kα radiation (1.54 Å) generated at an acceleration voltage of 40 kV and a current of 250 mA. After the PEO process, the corrosion resistance of the specimen was tested by subjecting the specimen to a salt immersion test (3.5 wt.% NaCl) for 120 h. Electrochemical impedance spectroscopy (EIS) and potentiodynamic polarization were utilized to evaluate the corrosion resistance of the oxide layer on the $Mg_{95}Zn_{4.3}Y_{0.7}$ alloy with a Reference 600 potentiostat (Gamry Instruments, Warminster, PA, USA).

3. Results and discussion

3.1. Characteristics of the oxide layer on $Mg_{95}Zn_{4.3}Y_{0.7}$ alloy

Fig. 1 shows surface and cross-sectional images of the oxide layer on $Mg_{95}Zn_{4.3}Y_{0.7}$ alloy coated in the electrolyte containing $K_4P_2O_7$. As shown in Fig. 1(a)–(c), the oxide layers on the $Mg_{95}Zn_{4.3}Y_{0.7}$ alloy samples exhibited the typical surface morphology of materials treated with the PEO process regardless of the thickness of the layer, i.e., dense crater-like microstructures with some round shrinkage pores observed in the crater centers. For the 10 μm oxide layer, small pores of 1–2 μm in diameter were observed on the oxide surface. The pore size on the surface of the oxide layer increased as the processing time increased. The 30 μm oxide layer exhibited some cracks and small irregular pores of 1–2 μm in diameter, with occasional coarse pores of ~5 μm (Fig. 1(c)). In general, the oxide layer produced on the Mg alloy samples by the PEO process comprised two different layers: an outer porous layer and a very thin inner barrier layer (100–300 nm). As shown in Fig. 1(d)–(f), the pores only existed in the outer porous layer and interconnected with each other, but did not cross over through the inner barrier layer to the $Mg_{95}Zn_{4.3}Y_{0.7}$ alloy substrate, irrespective of the thickness of the oxide layer. These morphologies were not much different from those of oxide layers coated on bulk Mg and Mg alloys.

The X-ray diffraction (XRD) patterns of the oxide layer of the $Mg_{95}Zn_{4.3}Y_{0.7}$ alloy coated using the electrolyte containing $K_4P_2O_7$ are shown in Fig. 2. The oxide layer mainly consisted of MgO and Mg_2SiO_4. The peak of MgO increased as the coating thickness increased and the intensity of the peak of MgO was the highest in the 30 μm oxide layer. To determine whether phosphorus was present in the PEO coatings, EDS analysis was performed on the surface and cross-section of the oxide layer. The phosphorus content on the surface of the 30 μm oxide layer was 4.2–6.4 at.%. Fig. 3 shows the result of the EDS line scanning from the cross-section images of the oxide layer. The phosphorus was distributed uniformly throughout the oxide layer. This result indicates that the phosphate was successfully incorporated into the inner oxide layer during the PEO process. Liang et al. [12] reported that phosphorus from the electrolyte was indeed incorporated into the oxide coating during microarc oxidation and was present in the form of noncrystal phosphate.

3.2. Corrosion resistance behavior of the oxide layer on $Mg_{95}Zn_{4.3}Y_{0.7}$ alloy

The corrosion phenomenon and corrosion mechanism for the $Mg_{95}Zn_{4.3}Y_{0.7}$ alloy with different oxide thicknesses were evaluated by EDS testing in 3.5 wt.% NaCl solution. An AC impedance measurement was carried out for the oxide layer on

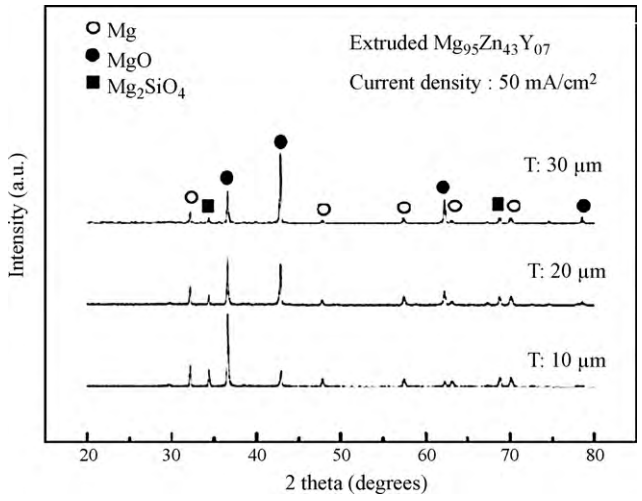

Fig. 2. XRD patterns of $Mg_{95}Zn_{4.3}Y_{0.7}$ alloy coated to 10 μm, 20 μm and 30 μm.

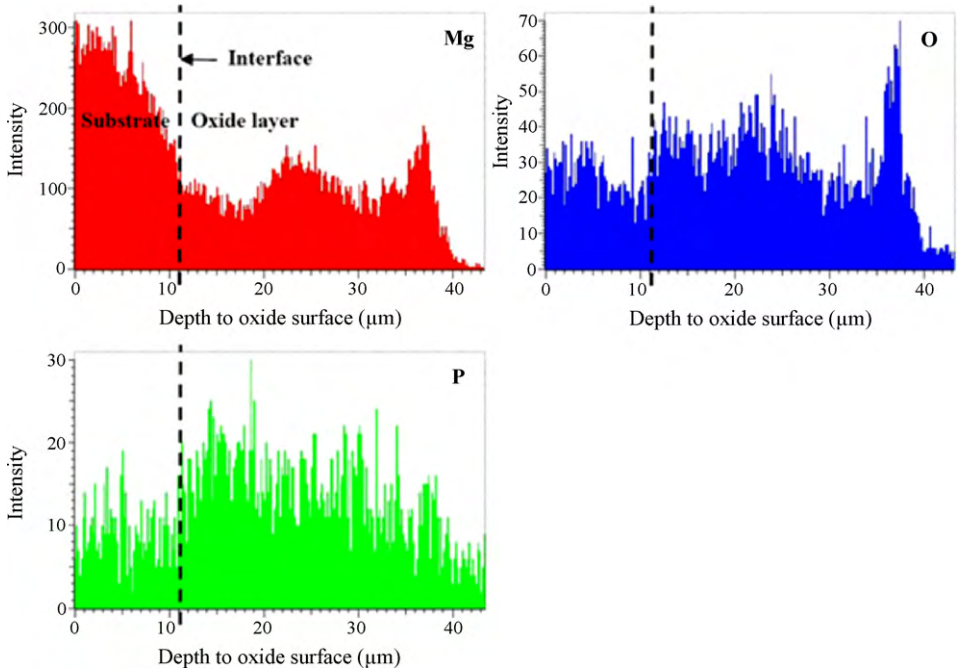

Fig. 3. Energy-dispersive spectra of $Mg_{95}Zn_{4.3}Y_{0.7}$ alloy coated to 30 μm.

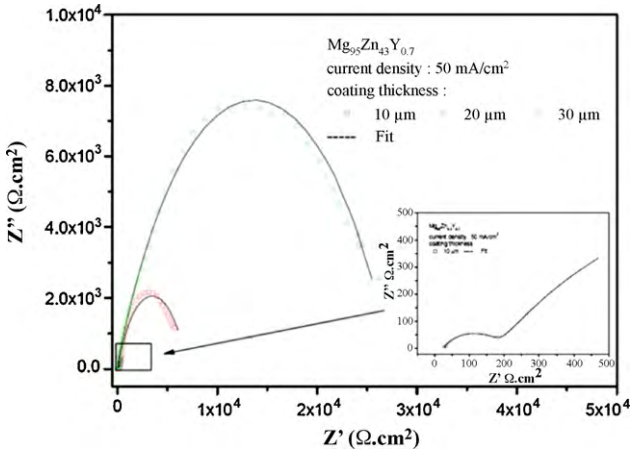

Fig. 4. Nyquist plot of oxide layer coated to 10 μm, 20 μm and 30 μm.

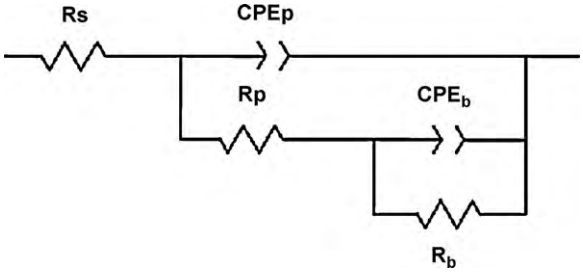

Fig. 5. Equivalent circuit used for fitting the impedance data of oxide layer.

the $Mg_{95}Zn_{4.3}Y_{0.7}$ alloy samples coated using electrolyte containing potassium pyrophosphate. The Nyquist plots for the 10 μm, 20 μm, and 30 μm oxide layers are shown in Fig. 4. It was found that the corrosion resistance of the sample coated to 30 μm was superior to those of the samples coated to 10 μm or 20 μm. In order to develop appropriate models for the impedance which fit the experimental data and allow extraction of the parameters that characterize the corrosion process, a simplified equivalent circuit on the oxide layer is proposed as shown in Fig. 5 [13]. In the equivalent circuit, the electrolyte resistance (R_s) is in series with the unit of the oxide layer system. R_p is the outer porous layer resistance paralleled with the constant phase element (CPE_p). The properties of the inner barrier layer are described by the resistance R_b in parallel with the CPE_b. Based on the equivalent circuit model in Fig. 5, the best fit for the Nyquist plot was determined and the fitting result is shown in Fig. 4 as solid lines passing through the test results. The corresponding values of the equivalent elements are listed in Table 1. It has been reported that the low frequency range of an impedance diagram characterizes the inner layer properties and the high frequency range reflects those of the outer layer [14,15]. The fitting results show that the resistance of thin inner barrier layer is higher than the corresponding value of the outer porous layer. Although the barrier layer of the Mg alloys was very thin, it could play an important role in corrosion resistance. Furthermore, the phosphate in the oxide layer has been previously reported as having a favourable influence on the corrosion resistance of Mg alloys [16].

The results of the 120 h immersion test for are shown in Fig. 6. Severe filiform corrosion was observed on the surface of the uncoated $Mg_{95}Zn_{4.3}Y_{0.7}$ alloy sample. Pitting and filiform corrosion occurred on the surface of the sample with the 10 μm coating. By

Table 1
Equivalent circuit data of 10 μm, 20 μm, and 30 μm oxide layers.

Thickness (μm)	R_s (Ω·cm^2)	CPE_p (F/cm^2)	CPE_p-P	R_p (Ω·cm^2)	R_b (Ω·cm^2)	CPE_b (F/cm^2)	CPE_b-P
10	27.64	9.45E−6	0.72	1.63E2	2.08E3	5.82E−4	0.66
20	16.47	2.19E−6	0.68	5.91E2	6.86E3	7.31E−6	0.69
30	17.57	1.13E−7	0.86	1.79E3	2.57E4	1.58E−6	0.6

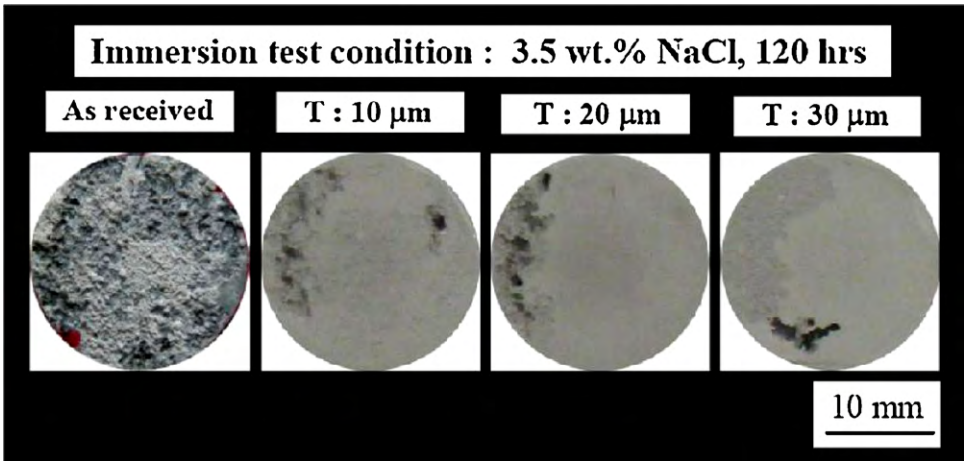

Fig. 6. Appearance of coated $Mg_{95}Zn_{4.3}Y_{0.7}$ alloy after salt spray test (120 h).

contrast, the sample with a 30 μm coating showed only localized pitting corrosion. Thus, the best corrosion resistance was observed in the sample with a 30 μm coating in the electrolyte containing potassium pyrophosphate.

4. Conclusions

The study has investigated the application of the PEO process to the coating of $Mg_{95}Zn_{4.3}Y_{0.7}$ alloy coated with different thickness of oxide layers using an electrolyte containing potassium pyrophosphate. Oxide layers were successfully formed on PM-processed $Mg_{95}Zn_{4.3}Y_{0.7}$ alloy samples, and the morphology of the oxide layers was not much different from that of oxide layers coated on bulk Mg alloys. The corrosion resistance of $Mg_{95}Zn_{4.3}Y_{0.7}$ alloy synthesized by the PEO process relied on the thickness of the oxide layer and the presence of the phosphate compound. The corrosion behavior of PM-processed $Mg_{95}Zn_{4.3}Y_{0.7}$ alloy was successfully described through electrochemical analysis, and the corrosion resistance of the oxide layer was confirmed through immersion testing.

Acknowledgements

This work was supported by the National Research Foundation (Grant No. 2009-0079807), and the Center for Advanced Materials Processing of the 21st Century Frontier R&D Program (Grant No. KRF-2007-357-d00136).

References

[1] C.S. Lin, Y.C. Fu, J. Electrochem. Soc. 153 (2006) B417–B424.
[2] S.H. Kim, D.H. Kim, N.J. Kim, Mater. Sci. Eng. A 226–228 (1997) 1030–1034.
[3] M. Suzuki, T. Kimura, J. Koike, K. Maruyama, Scripta Mater. 48 (2003) 997–1002.
[4] Y. Zhang, J. Chen, G.L. Chen, X.J. Liu, Appl. Phys. Lett. 89 (2006) 131904(1)–131904(3).
[5] X.T. Guo, P.J. Li, Y.H. Xiong, S.X. Liu, D.B. Zeng, J. Mater. Eng. 8 (2004) 60–64 (in Chinese).
[6] I.J. Kim, D.H. Bae, D.H. Kim, Mater. Sci. Eng. A 359 (2003) 313–318.
[7] M. Matsuda, S. Ii, Y. Kawamura, Y. Ikuhara, M. Nishida, Mater. Sci. Eng. A 386 (1–2) (2004) 447–452.
[8] H.J. Chae, T.S. Kim, Y.D. Kim, J. Alloys Compd., submitted.
[9] A.L. Yerokhin, X. Nie, A. Leyland, A. Matthews, S.J. Dowey, Surf. Coat. Technol. 122 (1999) 73–93.
[10] M.H. Lee, E.K. Park, T.G. Woo, I.S. Park, Y.M. Yoon, K.W. Seol, J. Kor. Inst. Met. Mater. 46 (2008) 747–755.
[11] Q. Cai, L. Wang, B. Wei, Q. Liu, Surf. Coat. Technol. 200 (2006) 3727–3733.
[12] J. Liang, B.G. Guo, J. Tian, H.W. Liu, J.F. Zhou, W.M. Liu, T. Xu, Surf. Coat. Technol. 199 (2005) 121–126.
[13] D.Y. Hwang, Y.M. Kim, D.Y. Park, B. Yoo, D.H. Shin, Electrochim. Acta 54 (2009) 5479–5485.
[14] F. Mansfeld, M.W. Kendig, J. Electrochem. Soc. 135 (1988) 828–833.
[15] S.C. Chung, J.R. Cheng, S.D. Chiou, Corros. Sci. 42 (2000) 1249–1268.
[16] H. Luo, Q. Cai, B. Wei, B. Yu, D. Li, J. He, Z. Liu, J. Alloys Compd. 464 (2008) 537–543.